

RADIO PROPER MOTIONS AND A SEARCH FOR THE ORIGIN OF PSR B1849+00

L. F. Rodríguez^{1,2}, S. A. Dzib³, L. A. Zapata¹ and L. Loinard¹

Draft version: August 16, 2024

RESUMEN

Hasta ahora no ha sido posible obtener el movimiento propio de PSR B1849+00 con técnicas de sincronización o imágenes de VLBI debido a la fuerte dispersión en su línea de visión. Presentamos un análisis de datos del archivo del Very Large Array en épocas de 2012 a 2022 que indican un movimiento propio total de 23.9 ± 5.5 mas yr $^{-1}$ hacia el suroeste. Después de corregir por el movimiento propio producido por la rotación galáctica encontramos una velocidad transversal peculiar de $\simeq 740$ km s $^{-1}$. Buscamos infructuosamente en la trayectoria pasada del pulsar por una remanente de supernova asociada. En particular, W44 está en esta trayectoria pero su distancia es diferente a la de PSR B1849+00.

ABSTRACT

Until now it has not been possible to obtain the proper motions of PSR B1849+00 with timing techniques or VLBI imaging given the enhanced interstellar scattering along its line of sight. We present an analysis of archive Very Large Array observations at epochs from 2012 to 2022 that indicates a total proper motion of 23.9 ± 5.5 mas yr $^{-1}$ toward the southwest. After correction for the proper motions produced by galactic rotation, we find a peculiar transverse velocity of $\simeq 740$ km s $^{-1}$. We searched unsuccessfully along the past trajectory of the pulsar for an associated supernova remnant. In particular, W44 is in this trajectory but its distance is different to that of PSR B1849+00.

Key Words: Proper motions (1295) — Radio astrometry (1337) — Radio pulsars (1353)

1. INTRODUCTION

The positions and proper motions of hundreds of pulsars have been determined using the analysis of pulsar timing residuals (e.g. Hobbs et al. 2004) and Very Long Baseline Interferometry (VLBI) imaging (e.g. Deller et al. 2019). However, in some cases, the pulsar suffers strong scattering effects from plasma along the line of sight. This condition scatters the radio image of the pulsar up to arcsec angular dimensions, ruling out the possibility of VLBI imaging. For some sources it has been possible to make images with connected interferometers (i.e. the Very Large Array), since these observations do not

¹Instituto de Radioastronomía y Astrofísica, UNAM, México.

²Mesoamerican Center for Theoretical Physics, UNACH, México

³Max-Planck-Institut für Radioastronomie, Germany

resolve out the scattered emission (e.g. Dzib et al. 2018). Multiple examples of pulsars whose proper motions have been determined with the Very Large Array are given by Brisken et al. (2003). The presence of inhomogeneous plasma in the line of sight also limits the timing method by broadening the pulses to a level that makes timing experiments difficult or impossible.

PSR B1849+00 (PSR J1852+00) is a pulsar that has a period of 2.18 s and a characteristic age of $10^{5.55}$ yr (Taylor et al. 1993). It is located in a region of enhanced line-of-sight interstellar scattering (Lazio 2004) that makes it one of the most heavily scattered pulsar known, with a pulse broadening time of 0.22 seconds at 1.4 GHz (Löhmer et al. 2001). It has a large dispersion measure, $\text{DM} = 787 \text{ cm}^{-3} \text{ pc}$ (Han et al. 2016). Only seven of the 228 pulsars studied by these authors have larger dispersion measures.

In this paper we present an analysis of archive Very Large Array data with the goal of determining the proper motions of PSR B1849+00 and possibly advance in our understanding of the supernova that created this pulsar.

2. VLA OBSERVATIONS

We searched unsuccessfully in the archives of the Karl G. Jansky VLA of NRAO⁴ for observations made in the highest angular resolution A configuration pointing toward PSR B1849+00. We found, however, several good quality A configuration observations made in the L-band (1-2 GHz) with the phase center at the position of the gain calibrator J1851+0035. Even when J1851+0035 is located at $\sim 11'$ from PSR B1849+00 we could obtain images of good quality over the full extent of the primary beam ($\sim 30'$). This was possible because the Jansky VLA records the continuum data in narrow channels (2 MHz), that do not produce significant bandwidth smearing. For all observations the position of J1851+0035 used was the updated position given in the VLA Calibrator Manual, $\text{RA(J2000)} = 18^h 51^m 46\rlap{.}^s 7217$; $\text{DEC(J2000)} = 00^\circ 35' 32\rlap{.}'' 414$. The data were calibrated in the standard manner using the CASA (Common Astronomy Software Applications; McMullin et al. 2007) package of NRAO and the pipeline provided for VLA⁵ observations. We made images using a robust weighting (Briggs 1995) of 0 to optimize the compromise between angular resolution and sensitivity. All images were also corrected for the primary beam response. Finally, the images were also corrected for wide-field effects using the gridding option *widefield* with 10×10 subregions in the task TCLEAN (Rodriguez et al. 2023).

3. DISCUSSION

In Table 1 we list the five projects found, indicating the name of the project, its mean epoch, frequency, synthesized beam, and flux density. We finally give the position of PSR B1949+00 for each epoch. In Figure 1 we

⁴The National Radio Astronomy Observatory is a facility of the National Science Foundation operated under cooperative agreement by Associated Universities, Inc.

⁵<https://science.nrao.edu/facilities/vla/data-processing/pipeline>

TABLE 1
PARAMETERS OF THE JANSKY VLA OBSERVATIONS

| Project | Mean Epoch | ν (GHz) | Synthesized Beam | Flux Density (mJy) | Position of PSR B1849+00 | |
|---------|------------|-------------|--|--------------------|--|--|
| | | | | | RA(J2000) ^a | DEC(J2000) ^b |
| 12B-225 | 2012.779 | 1.50 | 1. ^{''} 47×1. ^{''} 21; +20°6 | 3.51±0.33 | 27 ^h 499±0 ^s 002 | 01. ^{''} 91±0. ^{''} 03 |
| 14A-404 | 2014.362 | 1.52 | 2. ^{''} 25×1. ^{''} 60; -44°4 | 4.74±0.20 | 27 ^h 502±0 ^s 002 | 01. ^{''} 83±0. ^{''} 02 |
| 15A-301 | 2015.630 | 1.50 | 2. ^{''} 05×1. ^{''} 35; -48°4 | 6.04±1.00 | 27 ^h 507±0 ^s 007 | 01. ^{''} 80±0. ^{''} 05 |
| 19A-386 | 2019.647 | 1.57 | 1. ^{''} 39×1. ^{''} 21; +24°8 | 3.92±0.32 | 27 ^h 494±0 ^s 004 | 01. ^{''} 80±0. ^{''} 03 |
| 22A-097 | 2022.474 | 1.52 | 2. ^{''} 29×1. ^{''} 32; +65°3 | 2.42±0.21 | 27 ^h 486±0 ^s 004 | 01. ^{''} 72±0. ^{''} 02 |

^aOffset from RA(J2000) = 18^h52^m00^s.

^bOffset from DEC(J2000) = +00°32'00".

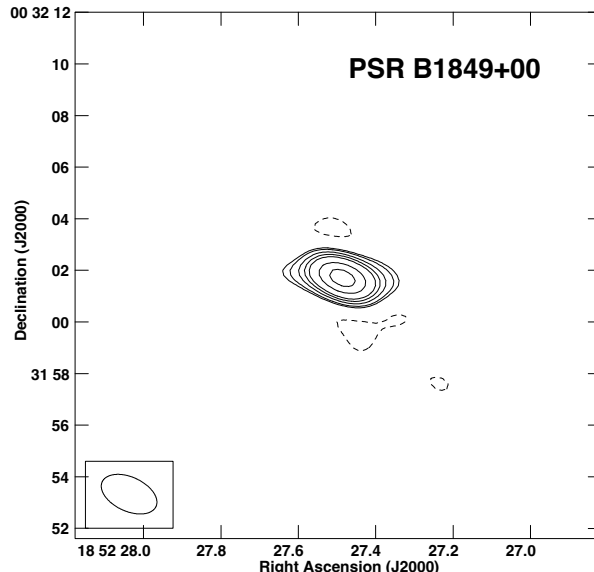


Fig. 1. Very Large Array contour image of PSR B1849+00 at 1.52 GHz for epoch 2022.474. Contours are -3, 3, 4, 6, 8, 10, 15, and 20 times 100 $\mu\text{Jy beam}^{-1}$, the rms noise in this region of the image. The synthesized beam ($2.^{\prime\prime}29 \times 1.^{\prime\prime}32; +65^{\circ}3$) is shown in the bottom left corner of the image.

show a contour image of the source from project 22A-097. In Figure 2 we present the positions as a function of time for PSR B1949+00. In Table 2 we give the equatorial proper motions obtained from a least-squares fit to the positions shown in Figure 2. In this Table we can see that PSR B1949+00 has a statistically significant equatorial total proper motion ($4.3-\sigma$).

The weighted mean flux density and weighted mean standard deviation at 1.5 GHz over the five epochs are 3.7 ± 1.1 mJy for PSR B1949+00. The spectral index can be used to further define the nature of the radio source. Kijak et al. (2011) report a spectral index of $\alpha = -2.4$ for this source, a steep value characteristic of pulsars (e.g. Taylor et al. 1993; Maron et al. 2000).

TABLE 2
POSITION AND PROPER MOTIONS OF PSR B1849+00

| Position ^a | | Equatorial Proper Motions ^d | | | | | Corrected Galactic Proper Motions ^d | | |
|--|--------------------------------------|--|-------------|---------------|-----------------|----------------|--|---------------|-----------------|
| RA(J2000) ^b | DEC(J2000) ^c | $\mu_{RA}\cos(\text{DEC})$ | μ_{DEC} | μ_{TOTAL} | PA ^e | $\mu_l\cos(b)$ | μ_b | μ_{TOTAL} | PA ^e |
| 27 ^h 518±0 ^h 007 | 02 ^m 06±0 ^m 06 | -19.1±6.4 | -14.4±3.2 | 23.9±5.5 | 233° ± 9° | -14.6±5.8 | +10.4±4.2 | 17.9±5.3 | 305° ± 15° |

^aFor epoch 2000.0.

^bOffset from RA(J2000) = 18^h52^m00^s.

^cOffset from DEC(J2000) = +00°32'00".

^dIn mas yr⁻¹.

^ePosition angle of the proper motion vector in the respective coordinates.

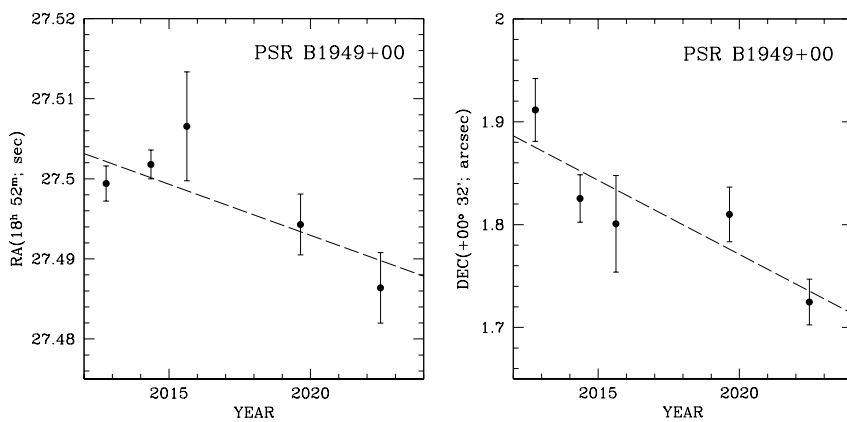


Fig. 2. (Left) Right ascension and (right) declination of PSR B1849+00 as a function of time. The dashed lines indicate the least squares fit for each parameter. The resulting proper motions are given in Table 2.

4. THE TRANSVERSE VELOCITY OF PSR B1849+00

The distance of PSR B1849+00 has been estimated by several groups. We weight-averaged the results of Cordes & Lazio (2003), Verbiest et al. (2012), Yao et al. (2017), Pynzar (2020) and Kütükçü et al. (2022), listed in Table 3, to obtain a value of 8.6 ± 1.7 kpc.

The total proper motions of PSR B1949+00 have to be corrected for the proper motion contribution due to the kinematics of the Galaxy in order to obtain the peculiar proper motions. We use a distance from the Sun to the center of the Galaxy of 8.15 kpc and a circular rotation velocity at the Sun of 236 km s⁻¹ (Reid et al. 2019). We also assume a flat rotation curve outside the tangent point (with a galactocentric distance of 4.6 kpc in the direction of the pulsar) and that the H I disk of the Galaxy has an outer radius of 13.4 kpc (Goodwin, Gribbin, & Hendry 1998). In Figure 3 we show the proper motion in galactic longitude for a circular Galactic orbit as a function of distance in the direction of PSR B1949+00. At the distance of the pulsar, 8.6 kpc, a galactic longitude proper motion of -6.9 mas yr⁻¹ is expected. We have corrected the galactic proper motions of PSR B1949+00 for this effect to obtain the values given in Table 2. This correction reduces the total proper

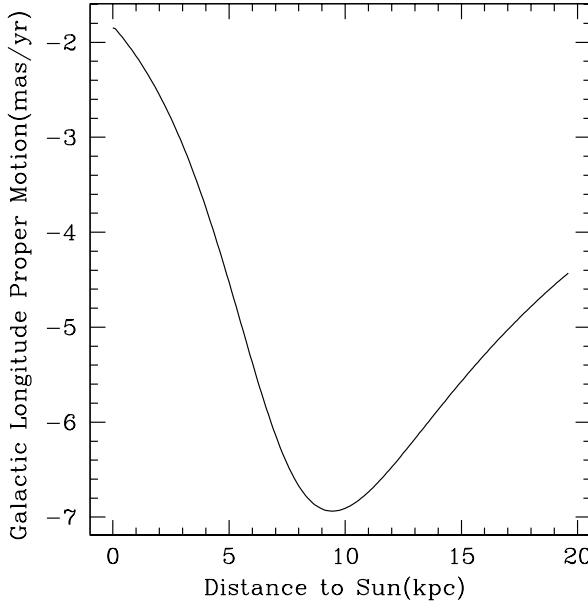


Fig. 3. Galactic longitude proper motion in the direction of PSRB1849+00 as a function of distance to the Sun. This theoretical curve is based on the Galactic model for circular motion described in the text.

TABLE 3
DISTANCE ESTIMATES TO PSR B1849+00

| Distance(kpc) | Method | Reference |
|---------------|--------------------------|------------------------|
| 8.4±1.7 | Dispersion measure model | Cordes & Lazio (2003) |
| 8.0±2.0 | HI absorption | Verbiest et al. (2012) |
| 7.0±1.0 | HI absorption | Yao et al. (2017) |
| 10.7± 0.9 | Dispersion measure model | Pynzar et al. (2020) |
| 7.0±1.5 | Dispersion measure model | Kütükcü et al. (2022) |

motion from 23.9 mas yr^{-1} to 17.9 mas yr^{-1} . This is the peculiar proper motion of the pulsar.

At the distance of 8.6 kpc the corrected total proper motion implies a peculiar velocity of $740\pm220 \text{ km s}^{-1}$ in the plane of the sky. The large error comes from propagating the errors in the proper motion and in the distance. The Australia Telescope National Facility Pulsar Catalogue (Manchester et al. 2005) lists a total of 294 pulsars with reported transverse velocities. Of these pulsars, 15 (5%) equal or exceed 740 km s^{-1} .

5. THE POSSIBLE ORIGIN OF PSR B1849+00

In Figure 4 we plot the position and proper motion of PSR B1849+00, superposed on a GLOSTAR image at 5.8 GHz (Medina et al. 2019; Brunthaler et al. 2021; Medina et al. 2024). In this image we also mark with circles supernova remnants and candidate supernova remnants in the region.

The sources best aligned with the past trajectory of PSR B1849+00 are the W44 remnant and the supernova remnant candidate G34.524-0.761. Taking the characteristic age of $10^{5.55}$ yr and the corrected total proper motion given in Table 2, we find that assuming a ballistic motion the origin would be located at $\sim 1^\circ 77$ to the NE of its present position. The supernova W44 is located at $1^\circ 16$ to the NE of PSR B1849+00 and sounds like an interesting possibility since pulsar characteristic ages could depart importantly from the true age of the pulsar (Suzuki et al. 2021).

However, the distance of W44 appears to be well established at $\simeq 3$ kpc (Radhakrishnan et al. 1972; Caswell et al. 1975; Cox et al. 1999; Su et al. 2014; Wang et al. 2020). The first four groups used HI absorption observations and a model of the Galactic kinematics, while the last one used the extinction to red clump stars (Paczyński & Stanek 1998) probably associated with the supernova. This significantly different distance seems to rule out an association of W44 with PSR B1849+00. In any case, it would be valuable to estimate the distance to W44 doing parallax measurements of the OH 1720 MHz masers associated with it. Also W44, whose age is estimated to be $\simeq 20,000$ yr (Smith et al. 1985; Cox et al. 1999; Giuliani et al. 2011), seems to be much younger than the pulsar and this result also gravitates against an association. The supernova age is estimated from observations of its size, expansion rate, and the properties of the surrounding interstellar medium.

The distance to G34.524-0.761 is not yet determined. This source has a spectral index of -0.9 and exhibits a 10% degree of linear polarization (Dokara et al. 2023), supporting the supernova remnant interpretation. However, as noted by these authors, its filamentary morphology suggests that it is probably a fragment of a much larger faint remnant. We conclude that we cannot associate clearly a supernova remnant with PSR B1849+00. It is probable that the related supernova remnant has mixed with the interstellar medium and is no longer detectable.

The Next Generation VLA (Murphy et al. 2018), with its unprecedented sensitivity and high angular resolution will be the ideal instrument for the study of the proper motions of pulsars whose image and pulses are scattered by inhomogeneous plasma in the line of sight.

6. CONCLUSIONS

- 1) We analyzed archive VLA observations of the pulsar PSR B1849+00 to obtain its radio proper motions. At a distance of 8.6 kpc the resulting peculiar velocity in the plane of the sky is $\simeq 740$ km s $^{-1}$.

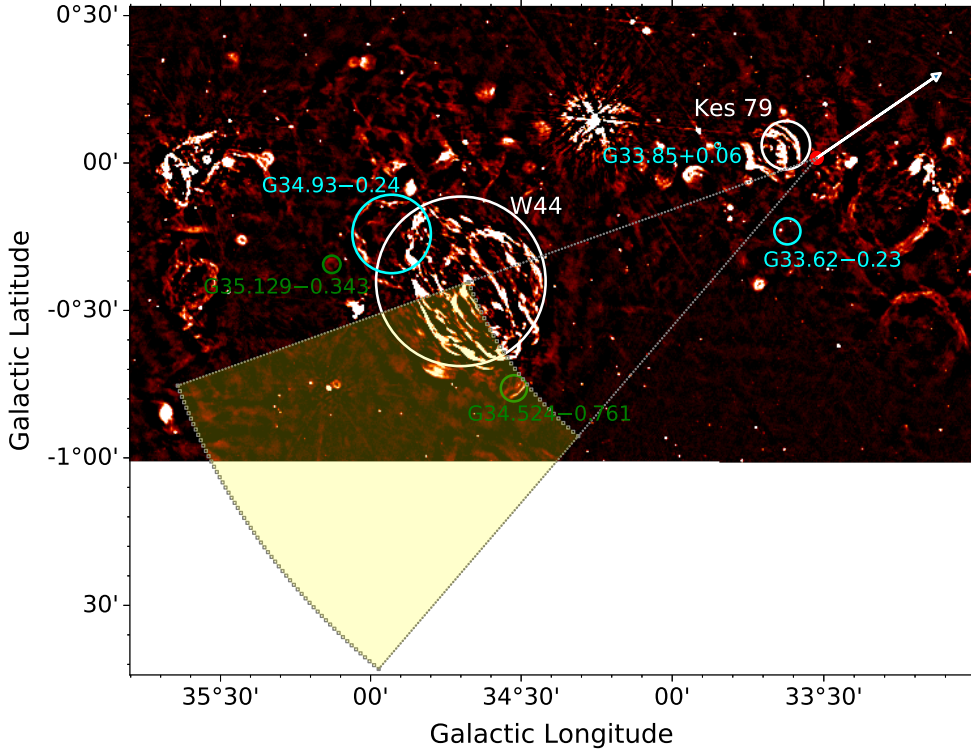


Fig. 4. Position (red dot) and proper motion of PSR B1849+00 for a period of 10^5 yr (white arrow) in galactic coordinates and superposed on a GLOSTAR image. The dashed lines indicate the $\pm 1\sigma$ angular range for the past trajectory of the pulsar. The dashed curved lines indicate the $\pm 1\sigma$ distance range for the origin of the pulsar assuming an age of $10^{5.55}$ yr, the characteristic age of the pulsar. These dashed lines define the most likely area in the sky for the origin of the pulsar, shown in yellow. The white circles indicate the position and extent of confirmed supernova remnants (Green 2022), while the green and cyan circles indicate candidate supernova remnants from Dokara et al. (2021) and Anderson et al. (2017), respectively.

2) We searched unsuccessfully along the past trajectory of PSR B1849+00 for a supernova remnant that could be associated with this pulsar. The bright supernova remnant W44 is in the past trajectory of the pulsar, but its distance is different. We suggest that the remnant that originated PSR B1849+00 has dissipated and is no longer detectable.

L.A.Z. acknowledges financial support from CONACyT-280775 and UNAM-PAPIIT IN110618, and IN112323 grants, México. L.L. acknowledges the support of DGAPA PAPIIT grant IN108324. L.F.R. acknowledges the financial support of DGAPA (UNAM) IN105617, IN101418, IN110618 and IN112417 and CONACyT 238631 and 280775-CF grant 263356. S.A.D. acknowledges the M2FINDERS project from the European Research Council (ERC) under the European Union's Horizon 2020 research and innovation programme (grant No 101018682).

REFERENCES

- Anderson, L. D., Wang, Y., Bihr, S., et al. 2017, A&A, 605, A58. doi:10.1051/0004-6361/201731019
- Briggs, D. S. 1995, American Astronomical Society Meeting Abstracts, 187, 112.02
- Brisken, W. F., Fruchter, A. S., Goss, W. M., et al. 2003, AJ, 126, 3090. doi:10.1086/379559
- Brunthaler, A., Menten, K. M., Dzib, S. A., et al. 2021, A&A, 651, A85. doi:10.1051/0004-6361/202039856
- Caswell, J. L., Murray, J. D., Roger, R. S., et al. 1975, A&A, 45, 239
- Cordes, J. M. & Lazio, T. J. W. 2003, astro-ph/0301598. doi:10.48550/arXiv.astro-ph/0301598
- Cox, D. P., Shelton, R. L., Maciejewski, W., et al. 1999, ApJ, 524, 179. doi:10.1086/307781
- Deller, A. T., Goss, W. M., Brisken, W. F., et al. 2019, ApJ, 875, 100. doi:10.3847/1538-4357/ab11c7
- Dokara, R., Brunthaler, A., Menten, K. M., et al. 2021, A&A, 651, A86. doi:10.1051/0004-6361/202039873
- Dokara, R., Gong, Y., Reich, W., et al. 2023, A&A, 671, A145. doi:10.1051/0004-6361/202245339
- Dzib, S. A., Rodríguez, L. F., Karuppusamy, R., et al. 2018, ApJ, 866, 100. doi:10.3847/1538-4357/aada07
- Goodwin, S. P., Gribbin, J., & Hendry, M. A. 1998, The Observatory, 118, 201
- Green, D. A., 2022, ‘A Catalogue of Galactic Supernova Remnants (2022 December version)’, Cavendish Laboratory, Cambridge, United Kingdom (available at “<http://www.mrao.cam.ac.uk/surveys/snrs/>”).
- Hobbs, G., Lyne, A. G., Kramer, M., et al. 2004, MNRAS, 353, 1311. doi:10.1111/j.1365-2966.2004.08157.x
- Han, J., Wang, C., Xu, J., et al. 2016, Research in Astronomy and Astrophysics, 16, 159. doi:10.1088/1674-4527/16/10/159
- Kijak, J., Lewandowski, W., Maron, O., et al. 2011, A&A, 531, A16. doi:10.1051/0004-6361/201014274
- Kütükçü, P., Ankay, A., Yazgan, E., et al. 2022, MNRAS, 511, 4669. doi:10.1093/mnras/stac346
- Lazio, T. J. W. 2004, ApJ, 613, 1023. doi:10.1086/423261
- Löhmer, O., Kramer, M., Mitra, D., et al. 2001, ApJ, 562, L157. doi:10.1086/338324
- Manchester, R. N., Hobbs, G. B., Teoh, A., et al. 2005, AJ, 129, 1993. doi:10.1086/428488
- Maron, O., Kijak, J., Kramer, M., et al. 2000, A&AS, 147, 195. doi:10.1051/aas:2000298
- Medina, S.-N. X., Urquhart, J. S., Dzib, S. A., et al. 2019, A&A, 627, A175. doi:10.1051/0004-6361/201935249
- Medina, S.-N. X., Dzib, S. A., Urquhart, J. S., et al. 2024, arXiv:2407.12585. doi:10.48550/arXiv.2407.12585
- Murphy, E. J., Bolatto, A., Chatterjee, S., et al. 2018, Science with a Next Generation Very Large Array, 517, 3. doi:10.48550/arXiv.1810.07524
- Paczynski, B. & Stanek, K. Z. 1998, ApJ, 494, L219. doi:10.1086/311181
- Pynzar, A. V. 2020, Astronomy Reports, 64, 681. doi:10.1134/S1063772920090036
- Radhakrishnan, V., Goss, W. M., Murray, J. D., et al. 1972, ApJS, 24, 49. doi:10.1086/190249

- Reid, M. J., Menten, K. M., Brunthaler, A., et al. 2019, ApJ, 885, 131. doi:10.3847/1538-4357/ab4a11
- Rodriguez, L. F., Yanza, V., & Dzib, S. A. 2023, arXiv:2311.14296. doi:10.48550/arXiv.2311.14296
- Smith, A., Jones, L. R., Watson, M. G., et al. 1985, MNRAS, 217, 99. doi:10.1093/mnras/217.1.99
- Su, H., Tian, W., Zhu, H., et al. 2014, Supernova Environmental Impacts, 296, 372. doi:10.1017/S1743921313009885
- Suzuki, H., Bamba, A., & Shibata, S. 2021, ApJ, 914, 103. doi:10.3847/1538-4357/abfb02
- Taylor, J. H., Manchester, R. N., & Lyne, A. G. 1993, ApJS, 88, 529. doi:10.1086/191832
- Verbiest, J. P. W., Weisberg, J. M., Chael, A. A., et al. 2012, ApJ, 755, 39. doi:10.1088/0004-637X/755/1/39
- Wang, S., Zhang, C., Jiang, B., et al. 2020, A&A, 639, A72. doi:10.1051/0004-6361/201936868
- Yao, J. M., Manchester, R. N., & Wang, N. 2017, ApJ, 835, 29. doi:10.3847/1538-4357/835/1/29

Sergio A. Dzib: Max-Planck-Institut für Radioastronomie, Auf dem Hügel 69, D-53121 Bonn, Germany.

Laurent Loinard, Luis F. Rodríguez & Luis A. Zapata: Instituto de Radioastronomía y Astrofísica, Universidad Nacional Autónoma de México, Apartado Postal 3-72, 58090 Morelia, Michoacán, México (l.rodriguez@irya.unam.mx).